

Design of Nano-Composites for Ultra-High Strengths and Radiation Damage Tolerance

A. Misra¹, X. Zhang², M.J. Demkowicz³, R. G. Hoagland¹ and M. Nastasi¹,

¹ Los Alamos National Laboratory, MS K771, Los Alamos, NM 87545.

² Texas A&M University, College Station, TX.

³ MIT, Cambridge, MA.

ABSTRACT

The combination of high strength and high radiation damage tolerance in nanolaminate composites can be achieved when the individual layers in these composites are only a few nanometers thick and therefore these materials contain a large volume fraction associated with interfaces. These interfaces act both as obstacles to slip, as well as sinks for radiation-induced defects. The morphological and phase stabilities of these nano-composites under ion irradiation are explored as a function of layer thickness, temperature and interface structure. Using results on model systems such as Cu-Nb, we highlight the critical role of the atomic structure of the incoherent interfaces that exhibit multiple states with nearly degenerate energies in acting as sinks for radiation-induced point defects. Reduced radiation damage also leads to a reduction in the irradiation hardening, particularly at layer thickness of approximately 5 nm and below. The strategies for design of radiation-tolerant structural materials based on the knowledge gained from this work will be discussed.

KEYWORDS: Irradiation damage, dislocations, multilayers, interfaces

INTRODUCTION

The performance of structural materials in extreme environments of irradiation and temperature must be significantly improved to extend the reliability, lifetime, and efficiency of future nuclear reactors [1]. In reactor environments, damage introduced in the form of radiation-induced defects and helium results in embrittlement and dimensional instability. Therefore, the ability to control radiation-induced point defects and helium bubble nucleation and growth is a crucial first step to improving the mechanical properties of irradiated metals. This calls for novel approaches in designing structural materials that resist radiation damage while maintaining high strength and toughness. Using nanolayered metallic composites as model systems, we highlight how tailoring the length scales (layer thickness) and interface properties can provide insight into ways of designing radiation damage tolerant structural materials.

The experiments described here were conducted on sputter deposited Cu-Nb multilayers and single layer Cu and Nb samples using He⁺ ion implantation to cover a broad range of irradiation conditions and layer thicknesses as described below [2-5] (throughout this article, multilayers are designated by the individual layer thickness or one-half of the bilayer period. Thus, 2 nm multilayer refers to a sample with a bilayer period of 4 nm with 2 nm Cu and 2 nm Nb layers). Cu and Nb have a positive heat of mixing, very limited solid solubility, and no tendency to form intermetallic compounds. Thus, the interfaces between Cu and Nb layers are very distinct with little evidence of mixing. But irradiation and/or temperature can lead to morphological

instabilities. The spheroidization of layered structures upon thermal annealing is well known. However, our earlier work on vacuum annealing of Cu-Nb nanolayered composites did reveal remarkable thermal stability in these materials with no evidence of spheroidization up to 800 °C [6]. This observation formed the basis to explore the stability of nanolayered composite materials under irradiation conditions. Similarly, radiation may destroy the geometrical arrangement of the layered structure because the flow of radiation-induced point defects into an interface changes its atomic configuration, perturbing its shape from flat to meandering. Such undulations provide an opportunity for adjacent nanometer-spaced interfaces to react and pinch off. Because the stability of the layered structure relies upon the planarity of the interfaces, such reactions can destabilize the structure and trigger the onset of recrystallization. There is a competition between restoring forces acting to flatten the interface and the undulations induced by rapid adsorption of defects. Chemical and morphological stabilities of the interfaces are necessary factors in the design of nanolayered composites where interfaces are to act as sinks of radiation-induced defects.

RESULTS AND DISCUSSION

The results presented below are organized to highlight the roles of interfaces in (i) suppression of helium bubble nucleation, (ii) retardation of helium bubble growth at elevated temperatures, (iii) reducing irradiation hardening, and (iv) producing high strength materials.

Delayed Nucleation of Bubbles in Nanolayered Composites

The equilibrium solid solubility of helium in metals such as Cu and Nb is extremely low, on the order of parts per billion or smaller. For helium concentrations above the solubility limit, helium tends to cluster and precipitate in the form of bubbles. However, the solubility of helium is expected to be higher at grain boundaries and interphase interfaces. As an upper bound, if we estimate that one monolayer of helium can be in solution at an interface, then for a multilayer with an individual layer thickness of 2 nm (approximately 10 atomic layers), solubility of the composite is effectively on the order of several atomic %.

A summary of experiments performed in our team to document bubble nucleation in Cu-Nb multilayers is presented in table 1. Ion implantation results in a non-uniform concentration profile of the implanted species with a maximum in concentration occurring at a depth that depends on the implantation energy. Note that implanted helium doses of 6×10^{16} /cm² at 33 keV and 1×10^{17} /cm² at 150 keV produce equivalent maximum helium concentrations, but at different depths of 120 nm and 450 nm respectively. For these room temperature implantations, the doses we used resulted in two different maximum helium concentrations: (i) 5 at.% in Cu and 7 at.% in Nb, and (ii) 13 at.% in Cu and 21 at.% in Nb. At the 5-7% maximum He concentration, no bubbles were detected in through-focus transmission electron microscopy (TEM) images in the 2.5 nm Cu-Nb multilayers. Also, high-resolution TEM imaging revealed no amorphization or gross changes in interface structure indicating lack of any significant ion-beam mixing between Cu and Nb. However, monolithic films and 100 nm multilayers exhibited 1-2 nm size bubbles. At higher doses (> 13 at.% helium in Cu), bubbles are observed at all layer thicknesses. At the very smallest layer thickness (< 5 nm), helium bubbles were found to decorate the interfaces. In all cases of bubbles nucleated at room temperature, the bubble size was on the order of 1-2 nm.

Retarded Growth of Bubbles

The room temperature implanted samples that had > 13 at.% peak helium concentration and exhibited the 1-2 nm size bubbles were subjected to vacuum annealing at 600 °C for an hour [2]. The monolithic films and the 40 nm multilayers exhibited unstable bubble growth leading to blistering of the films. These blisters were relatively large, on the order of 1-5 μm in diameter, and most were cracked indicating release of helium from the samples. However, in the 5 nm multilayers the bubbles were much smaller. The bubble diameter was 5-10 nm, i.e., on the order of the layer thickness but no unstable growth leading to film blistering was observed. This observation highlights the unusual stability of the 5 nm multilayers subjected to extremely high doses of implanted helium and elevated temperatures.

In a different experiment [5], 33 keV $^4\text{He}^+$ ions were implanted at 490 °C to a total dose of $1 \times 10^{17} / \text{cm}^2$ in two different multilayers: 120 nm and 4 nm. In the 120 nm samples, large faceted bubbles, most exceeding 20 nm in diameter, were observed in the Cu layers. However, in the Nb layers the bubbles remained small, ~1-2 nm in diameter. In the 4 nm samples, the Nb layers still showed the 1-2 nm size bubbles but the size of the bubbles in the Cu layer was limited by the layer thickness of 4 nm. So, there emerges the very interesting behavior that, bubbles in the Cu layer grow to the thickness of the layer and stop at the interface.

In summary, we find that small He bubbles are the first to nucleate. Their sizes remain about 1-2 nm while their number density increases. Eventually the size of the bubbles increases with continued implantation of He, presumably because the He internal pressure in the small bubbles exceeds a critical pressure needed to initiate the punching of interstitials and/or Frank loops. For the conditions of implantation we chose in this study, this happens much more readily in the copper than in the niobium, consistent with the fact that the activation energy for point defect formation is much higher in Nb than in Cu. Thus, at a given temperature, a higher dose of helium is needed for bubble growth in Nb than in Cu.

Table 1 Summary of helium bubble nucleation as a function of room temperature implanted helium dose and layer thickness of multilayers

Irradiation conditions	Peak helium concentration	DPA	Were bubbles observed in TEM?
33 keV, $1.5 \times 10^{17} / \text{cm}^2$ [2]	13 at.% in Cu 21 at.% in Nb	Cu: 35 Nb: 15	5 nm Cu-Nb: yes 40 nm Cu-Nb: yes Single layer Cu: yes Single layer Nb: yes
*33 keV, $6 \times 10^{16} / \text{cm}^2$ or, *150 keV, $1 \times 10^{17} / \text{cm}^2$ [4]	5 at.% in Cu 7 at.% in Nb	Cu: 9 Nb: 6	2.5 nm Cu-Nb: no 100 nm Cu-Nb: yes Single layer Cu: yes

* Both of these conditions produced approximately the same level of maximum helium concentration and displacements per atom (DPA).

Suppression of Irradiation Hardening

Nanoindentation was used to measure the hardness of ion irradiated Cu-V and Cu-Nb multilayers. The hardness of ion-irradiated films was higher than as-deposited films but only for layer thickness greater than approximately 25 nm. At lower layer thickness the irradiation hardening was significantly decreased and was found to be negligible at layer thickness < 5 nm. For example, in the case of Cu-V, the measured hardness increase after irradiation decreased from ≈ 750 MPa at layer thickness of 200 nm to ≈ 50 -100 MPa at layer thickness of 2.5 nm. Radiation hardening in bulk metals caused by radiation-induced defects such as stacking fault tetrahedral, interstitial loops, helium bubbles, etc. In multilayers, as the density of radiation-induced defects and helium bubbles decreases with decreasing layer thickness, radiation hardening diminishes.

Atomistic Modeling

To elucidate the role of interfaces in reducing radiation damage in Cu-Nb multilayer composites, atomic-scale simulations have been carried out using embedded atom method (EAM) potentials [7]. These potentials were constructed by developing a cross-interaction term between well-tested single-element potentials for Cu [8] and Nb [9]. The resulting model of the Cu-Nb binary system correctly reproduces the known dilute enthalpies of mixing of these two elements as well as certain structural and energetic properties determined by first principles simulations using VASP [10]. The hard-core repulsive interactions between the element types modeled by this potential were obtained from the ZBL “universal” potential [11], which has been proven to accurately describe atomic interactions at short distances [12].

Collision cascade simulations were carried out on perfect crystalline FCC Cu and BCC Nb as well as on model Cu-Nb multilayer configurations constructed so as to obey the experimentally observed Kurdjumov-Sachs orientation relation [13]. The layer thicknesses in these configurations were ~ 4 nm, corresponding to those of the Cu-Nb multilayer composites that were He implanted and studied by TEM. The primary knock-on atom energies used in these simulations ranged from 0.5 to 2.5 keV, well below the approximate threshold energy for ion stopping due to electronic excitation [14]. These cascade simulations revealed a clear difference between the amounts of radiation damage—in the form of vacancy-interstitial (Frenkel) pairs—sustained by perfect crystalline Cu or Nb compared to the Cu-Nb multilayer composite. While all collision cascades occurring in the perfect crystals resulted in the creation of radiation damage, the number of point defects remaining after collisions in the vicinity of Cu-Nb interfaces was always markedly smaller. No point defects remain in the Cu or Nb layers neighboring a Cu-Nb interface as all the vacancies and interstitials created in the cascade core were quickly absorbed into the interface, where they recombined.

The unique ability of Cu-Nb interfaces to trap and recombine Frenkel pairs created during irradiation-induced collision cascades can be traced back to the unusual properties of interfacial point defects in Cu-Nb multilayer composites. One of the most noticeable differences between the behavior of such defects and the ones present in perfect crystalline environments of the corresponding element is the greatly reduced, by almost an order of magnitude, formation energy of interfacial point defects compared to the latter. Thus, vacancies and interstitials that migrate to the Cu-Nb interfaces are effectively trapped there and undergo accelerated recombination due to the enhanced diffusivity and effective size of interfacial point defects. The origin of the unusual properties of interfacial point defects such as low formation energies can be traced back to the structural characteristics of Cu-Nb interfaces, particularly their ability to support a multiplicity of distinct atomic arrangements [10] coexisting in the same interface.

Atomistic modeling is also useful in elucidating the resistance of the interface to the transmission of a single glide dislocation that is the critical unit process that largely determines the maximum strength achieved in nanoscale multilayers. For the case of Cu-Nb, it was shown that interfaces have low shear strength and large in-plane anisotropy of shear strength. This has significant implications for the interactions of glide dislocations, from either Cu or Nb crystal, with the interface. The stress field of a glide dislocation approaching the interface can exert enough stress to locally shear the 'weak' interface, resulting in its absorption and core spreading in the interface plane. Increasing the applied stress in the molecular dynamics simulation does not lead to compaction of the dislocation core and subsequent transmission across the interface. Thus, core spreading effectively pins a glide dislocation in the interface plane and so an incoherent interface that is 'weak' in in-plane shear can be a very strong barrier to slip transmission across interfaces. The weaker the interface, the larger the magnitude of core spreading, and hence, stronger the resistance to slip transmission. Transmission of slip across the interface appears to require multiple glide dislocations that absorb in the interface to react and emit glide dislocations across the interface. In the absence of any stress concentration from a pile-up, such processes may occur at applied stresses on the order of 2.5 - 3 GPa, consistent with the experimentally measured maximum flow strengths of Cu-Nb at $h < 5$ nm. The results are summarized in Fig. 1.

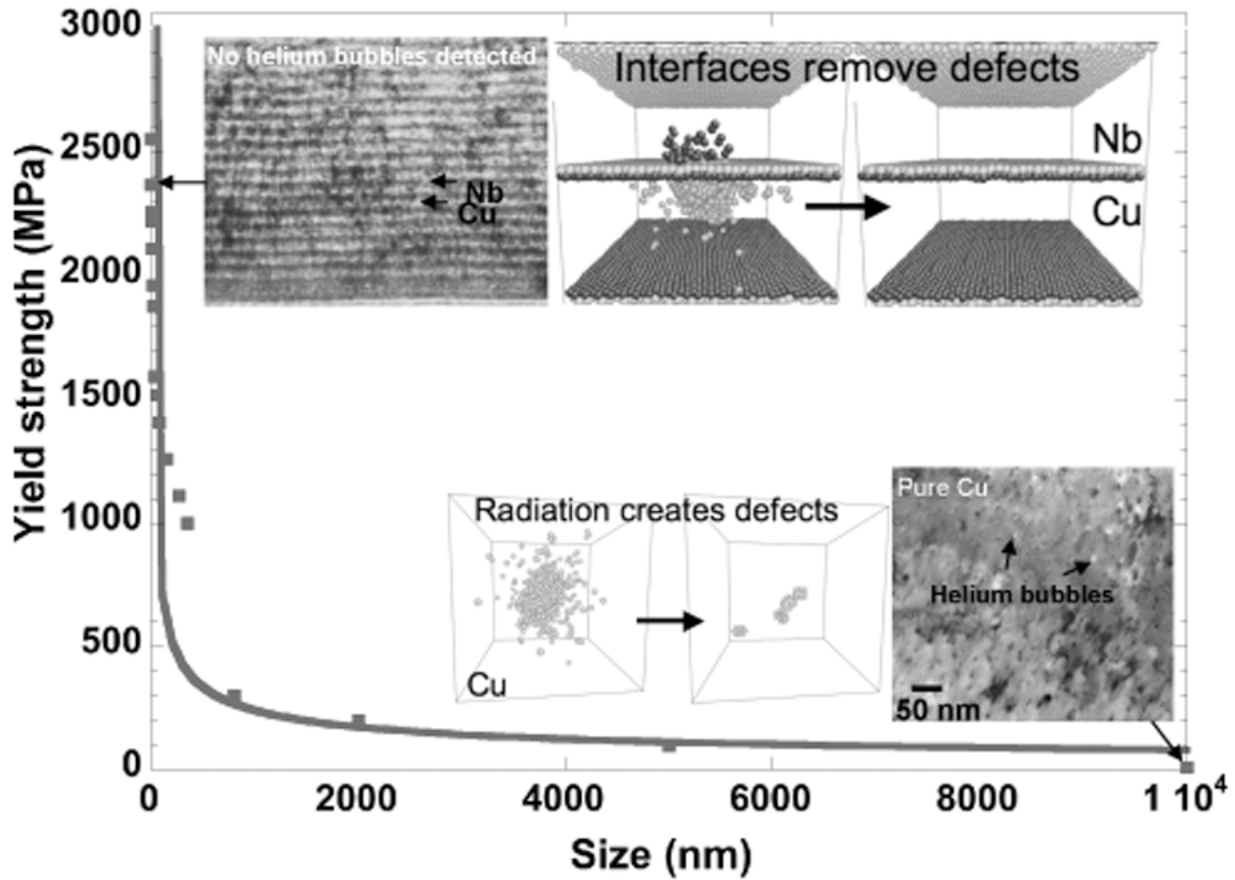


Figure 1: Interfaces act as obstacles to slip and sinks for radiation-induced defects. Nanolayered composites such as Cu-Nb provide orders of magnitude increase in strength and enhanced radiation damage tolerance compared to bulk materials. In the example shown, pure Cu and Cu-Nb (5 nm bilayer period) were irradiated at room temperature with He⁺ ions to a peak concentration of ≈ 5 at.%. While Cu sample showed defect agglomerates, no helium bubbles were resolved in through-focus imaging in a TEM. Atomistic modeling shows that radiation creates point defects that agglomerate in bulk materials but are attracted, absorbed and annihilated at incoherent interfaces in nanolayered composites. The arrows indicate the corresponding strength levels, prior to irradiation, for the pure Cu and Cu-Nb (5 nm bilayer period) samples.

SUMMARY

Nanolaminate composites can be designed via tailoring of length scales and atomic structure and energetics of interfaces to produce ultra-high strengths and enhanced radiation damage tolerance. This design philosophy was demonstrated using a model Cu-Nb nanolayered system. The flow strengths of these composites are on the order of 2.5 GPa at layer thickness of around 2

nm [15] and the best radiation damage tolerance is also observed at the smallest layer thicknesses of a few nanometers. It is well known that the strength increases with decreasing grain size (or, layer thickness) according to the Hall-Petch scaling law. However, the advantages for radiation tolerance are not realized until the relevant length scale, such as the layer thickness, is reduced to the nanometer range. It appears then that the enhanced radiation damage tolerance in nanocomposites is a consequence of short diffusion distance to the nearest sink. At the smallest sizes in the layered composites of a few nanometers, diffusion distances to sinks are short enough, due to the huge interface area in the material, to enable rapid removal of the point defects before they can form into relatively stable aggregates. Of course, the geometry of the nanostructured material must be stable under the extreme irradiation condition. As shown in this work on Cu-Nb nanolayers the layered geometry with flat interfaces extending throughout the sample thickness may provide a benefit in this regard as compared to nanostructured metals with equiaxed grain morphology [16, 17, 18] that may rapidly coarsen under irradiation at elevated temperatures. It should be possible to tailor the atomic structure and energetics of interfaces to provide the most effective sites for point defect trapping and annihilation [10, 19]. Based on the work so far it appears that the key attributes of interface are: (i) multiplicity of atomic arrangements with nearly degenerate energies, (ii) low formation energy of point defects, and (iii) delocalized point defect cores at interfaces such that the recombination distances are large. This is currently being explored via atomistic modeling and experiments in our laboratory. Specifically, the ongoing simulation research aims to create a theoretical framework for predicting the types of interfaces that also possess the structural characteristics observed in the model CuNb system and are therefore good candidates for use as point defect.

ACKNOWLEDGEMENTS

Research at LANL is supported by the Office of Basic Energy Sciences, Department of Energy. Authors acknowledge discussions with J.D. Embury, F. Spaepen and J.P. Hirth.

REFERENCES

1. BES Workshop report *Basic Research Needs for Advanced Nuclear Energy Systems* http://www.science.doe.gov/bes/reports/files/ANES_rpt.pdf
2. T. Hochbauer, A. Misra, K. Hattar and R.G. Hoagland, *J. Appl. Phys.*, **98**, 123516 (2005).
3. M.J. Demkowicz, Y.Q. Wang, R.G. Hoagland and O. Anderoglu, *Nucl. Instru. Methods B*, **261** (2007), 524.
4. X. Zhang, N. Li, O. Anderoglu, H. Wang, J.G. Swadener, T. Hochbauer, A. Misra and R.G. Hoagland, *Nucl. Instru. Methods B*, **261**, (2007), 1129.
5. K. Hattar, M.J. Demkowicz, A. Misra, and R.G. Hoagland, *Scripta Mater.*, **58** (2008) 541.
6. A. Misra, H. Kung and R.G. Hoagland, *Philos. Mag.*, **84**, 1021 (2004).
7. M. S. Daw and M. I. Baskes, *Physical Review B* **29**, 6443 (1984).
8. Y. Mishin, M. J. Mehl, D. A. Papaconstantopoulos, et al., *Physical Review B (Condensed Matter and Materials Physics)* **63**, 224106 (2001).
9. R. A. Johnson and D. J. Oh, *Journal Of Materials Research* **4**, (1989) 1195.
10. M. J. Demkowicz, J.P. Hirth and R. G. Hoagland, *Phys. Rev. Lett.*, **100**, (2008) 136102.
11. J. F. Ziegler, J. P. Biersack, and U. Littmark, *The stopping and range of ions in solids* (Pergamon, New York, 1985).

12. K. T. Kuwata, R. I. Erickson, and J. R. Doyle, Nuclear Instruments & Methods in Physics Research Section B-Beam Interactions with Materials and Atoms **201**, (2003) 566.
13. P. M. Anderson, J. F. Bingert, A. Misra, J.P. Hirth, Acta Materialia **51**, (2003) 6059.
14. G. J. Dienes and G. H. Vineyard, *Radiation effects in solids* (Interscience Publishers, New York, 1957).
15. A. Misra, J.P. Hirth and R.G. Hoagland, Acta Materialia, **53**, (2005) 4817.
16. N. Nita, R. Schaeublin, M. Victoria and R.Z. Valiev, Philos. Mag., **85**, (2005) 723.
17. M. Samaras, P.M. Derlet, H. van Swygenhoven and M. Victoria, Phys. Rev. Lett., **88**, (2002) 125505.
18. M. Rose, A.G. Balogh and H. Hahn, Nucl. Instru. Methods B, **127/128**, (1997) 119.
19. H.L. Hienisch, F. Gao and R.J. Kurtz, J. Nucl. Mater., **329-333**, (2004) 924.